European Conference on Optical Communication (ECOC) 2022 ©
Optica Publishing Group 2022

Interferometrically Coupled Reconfigurable Racetrack Resonator on Lithium Niobate-on-Insulator platform

Andreas Maeder[(1)], Fabian Kaufmann[(1)], Giovanni Finco[(1)], David Pohl[(1)], Jost Kellner[(1)], Xiyue Sissi Wang[(1)] and Rachel Grange[(1)]

[(1)] ETH Zürich, Department of Physics, Institute for Quantum Electronics, Optical Nanomaterial Group, 8093 Zurich, Switzerland maederan@phys.ethz.ch

Abstract *We exploit a thermo-optically tuned interferometric coupling scheme to relax fabrication tolerances on coupling segments of microresonators in lithium niobate-on-insulator. We achieve extinction ratios up to 34 dB and show tuning of resonance bandwidth between 15 and 45 pm while maintaining extinction above 15 dB. ©2022 The Author(s)*

Introduction

Resonators are widely used to increase light-matter interactions in many integrated optical platforms. There are countless demonstrations of high quality microresonators in silicon[1], silicon nitride[2], lithium niobate-on-insulator (LNOI)[3], and more. These resonators have a multitude of applications such as integrated lasers[4],[5], frequency combs[6],[7], and microring modulators[8],[9]. Also, resonators are often used to enhance nonlinear optical effects such as second harmonic generation[10],[11], optical parametric oscillation[12], or spontaneous four-wave-mixing[13].

LNOI is emerging as a versatile integrated photonics platform due to the steady improvement in nanofabrication processes[14]. Its high second order nonlinearity makes it an ideal candidate to explore nonlinear optical effects such as spontaneous parametric down-conversion.

Optical resonators can be used to boost the conversion efficiency of nonlinear-optical processes. For this, it is key that the resonators are in a regime close to critical coupling, where the extinction ratio (ER) is maximized[15]. To achieve this, the cavity coupling coefficient t has to be closely matched to the round-trip losses a. Resonator coupling in integrated photonics is almost exclusively achieved through directional couplers. By engineering the gap of the bus and resonator waveguide and the length of the coupling segment, the coupling coefficient is carefully tuned. However, these coupling segments are very sensitive to fabrication imperfections, specifically variations in waveguide height and coupling gap. Furthermore, these passive couplers stay in a fixed coupling regime once fabricated.

We relax these narrow fabrication tolerances by employing an interferometric coupling scheme[16] and by using thermo-optic phase shifters to actively tune an integrated racetrack resonators. Although there are several demonstrations of tunable resonators in LNOI[17]–[19], they exclusively focus on tuning the resonant wavelengths and not the ER, full width at half maximum (FWHM), or coupling regime.

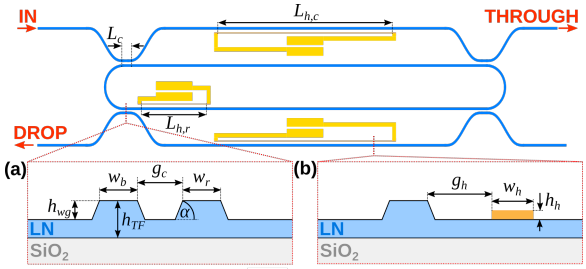

Fig. 1: Schematic representation of an integrated racetrack resonator in add-drop configuration. Coupling to the resonator is achieved using interferometric couplers with integrated TOPS to tune the phase-difference $\Delta\phi$. A third, shorter heater is included for resonance tuning. Two cuts show the cross-section of (a) the single evanescent coupling segments and (b) the metal-strip heater next to the bus waveguide, respectively.

In this study we design, fabricate, and characterise a reconfigurable integrated racetrack resonator on a 400 nm X-cut LNOI chip. Besides achieving thermo-optic tuning of the resonance position with an efficiency of 0.65 pm/mW, we also demonstrate critical coupling at different wavelengths in the S-, C- and L-band reaching extinction ratios up to 34 dB. By exploring the full tunability range of the individual couplers we measure an 8-fold difference between the minimum and maximum achievable bandwidth of the device, while simultaneously changing the extinction ratio between 0.35 and 21.9 dB. Finally, we tune the FWHM of a single resonance by a factor of 3 while mainting an extinction ratio above 15 dB. This is the first demonstration of independent extinction ratio and bandwidth tuning in an LNOI resonator, showing the potential of these devices as a versatile tool in integrated nonlinear photonics.

Operation Principle

The interferometric coupling scheme used here is schematically shown in figure 1. It is based on two identical coupling segments of length L_c. Each of these segments has a lumped coupling coefficient t_0 to the resonator. The couplers can be modelled as a single evanescent coupling segment with a coupling coefficient[20]

$$t = 2t_0(1 - t_0)(1 - \cos\Delta\phi), \quad (1)$$

where $\Delta\phi$ is the phase difference between the first and the second coupling segment. Depending on the value of t_0, the power coupling factor t can be tuned between t_{min} and 1. Figure 2(a) shows the theoretical extinction ratio of a resonance as a function of $\Delta\phi$ for a resonator in all-pass configuration. It can be observed that critical coupling can only be realised if $1 - t_{\text{min}} \geq a$. Note that also the resonance width changes simultaneously with $\Delta\phi$ as shown in figure 2(b).

By using a racetrack resonator in add-drop configuration with two interferometric coupling segments, we can achieve independent tuning. The critical coupling condition for a resonator in add-drop configuration is

$$t = 1 + t' - a, \quad (2)$$

where t and t' are the power coupling coefficients at the through and the drop side, respectively. For symmetric coupling segments (i.e. $t = t'$) this condition can never hold exactly since $0 < a < 1$.

With interferometric couplers however, we can tune t and t' such that condition (2) holds. Furthermore it is also possible to readjust them to get high extinction ratios at different FWHMs.

Design and Fabrication

To design the interferometric couplers, we use a Lumerical eigenmode expansion (EME) simulation to simulate the coupling segment consisting of two waveguides of widths w_b = w_r = 800 nm copropagating for a length L_c. The separation of the waveguides is g_c = 670 nm. The optical $|S_{12}|^2$ parameter is shown in figure 3(a). In the simulations we neglect contributions from the approaching bus-waveguide but only consider the parallel part of the segments. Since we are only interested in the tuning region around the critical coupling, we chose a coupling length of L_c = 28 µm corresponding to t_0 = 0.31. With typical propagation losses of 0.2 dB/cm in these devices, this suffices to be in the desired regime.

As phase-shifters in the interferometric couplers and for tuning the resonant wavelength, we use thermo-optic phase shifters (TOPS). They

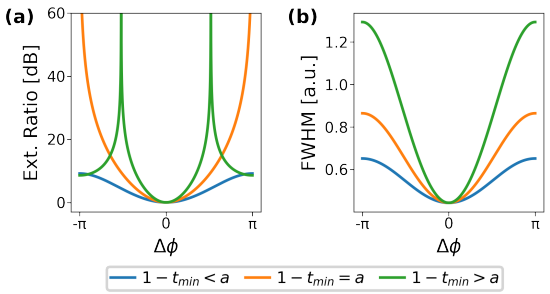

Fig. 2: Theoretically predicted resonance characteristics for a resonator in all-pass configuration using an interferometric coupler. For (a) the extinction ratio and (b) the FWHM three values for the base coupling coefficient t_0 are distinguished.

consist of a strip of platinum (Pt) with the following parameters: w_h = 3.1 µm, h_h = 100 nm and lengths $L_{h,b}$ = 960 µm for the interferometric couplers and $L_{h,r}$ = 360 µm for the resonator itself. The heater gaps are $g_{h,b}$ = 2.4 µm and $g_{h,r}$ = 2 µm respectively. $g_{h,r}$ is higher than $g_{h,b}$ to avoid ohmic losses in the resonator. The Pt-strips are connected with gold (Au) connections of 300 nm height and 20 µm width leading to negligible contributions to the overall resistance of the heater structure. A 3D finite element heat transfer model was used in conjunction with a 2D finite element mode simulation to predict a power for π phase-shift P_π = 421 mW for the interferometric coupler. Figure 3(b) shows the temperature profile generated at this power.

Figure 4(a) shows an optical microscope image of the fabricated device. The resonator consists of straight waveguides of length L = 2 mm and two half-circles with a radius R = 100 µm. The width for the bus and resonator waveguides is 800 nm. The waveguides were fabricated by electron-beam lithography followed by a 250 nm deep dry-etch in an ICP-RIE tool and have a width of 0.8 µm. Pt heaters and Au contacts were deposited using a double layer lift-off process. The TOPS show a resistance of 553 Ω and 556 Ω for the two coupler heaters and 790 Ω for the resonator heater.

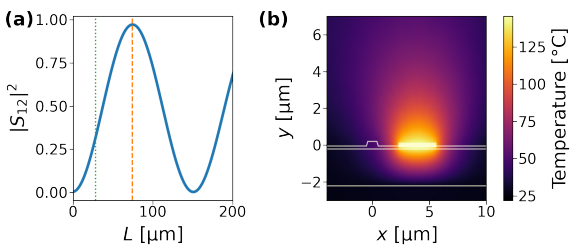

Fig. 3: (a) Simulation results of $|S_{12}|^2$ for two copropagating waveguide of 800 nm width and h_{wg} = 250 nm etch depth. The orange dashed line indicates the coupling length $L_{c,0}$ = 74.3 µm for complete power transfer. The green dotted line indicates L_c = 28 µm. (b) Simulated temperature profile for the thermo-optic phase-shifter used in the coupling segment.

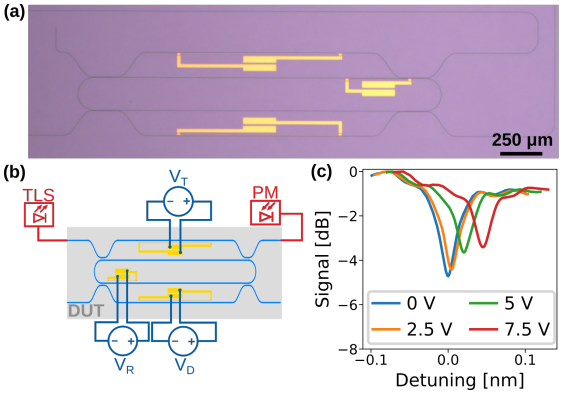

Fig. 4: (a) Optical Microscope image of the fabricated racetrack resonator. (b) The measurement setup used to characterise the device. (c) Measured resonance at λ_0 = 1561.2 nm for different voltage V_R applied to the TOPS at the resonator.

Experimental Results

The experimental setup used to characterise the fabricated device is shown in figure 4(b). We use tungsten needles to contact the Au connection pads of the TOPS. The sample is mounted on a copper holder held at constant temperature T_{amb} = 22 ℃ with a Peltier-element and a PID temperature controller. End-fire coupling with lensed fibers is used to couple light to the integrated circuit. A tunable laser source and a high dynamic range powermeter are used to measure transmission spectra while applying different voltages.

Figure 4(c) shows a resonance initially at λ_0 = 1561.17 nm at different applied voltages V_R to the TOPS in the resonator. The tuning efficiency of 0.65 pm/mW is of the same order of magnitude as previous reported values in LNOI ring-resonators[17] and could be improved by increasing the length of the metal strip to heat a bigger portion of the resonator waveguide. We also observe changes of the ER and FWHM which are due to thermal cross-talk to the couplers.

A resonance at λ_0 = 1520.0 nm was measured at different voltages V_T applied to the through side TOPS to investigate single side tuning characteristics of the device. Figures 5(a) and (b) show the ER and FWHM as a function of the applied voltage. The same measurement was repeated for different voltages V_D applied to the drop side coupler. With these applied voltages the resonance extinction ratio varies between 0.35 dB and 21.9 dB. Simultaneously the FWHM shows a factor 8 difference between the lowest and highest measured value. This confirms the working principle of the interferometric coupling scheme.

In figure 5(c), different resonances with extinction ratios beyond 27 dB are shown. These are achieved by applying different voltages V_D at the drop side coupler (refer to the figure caption for resonant wavelength and voltage values).

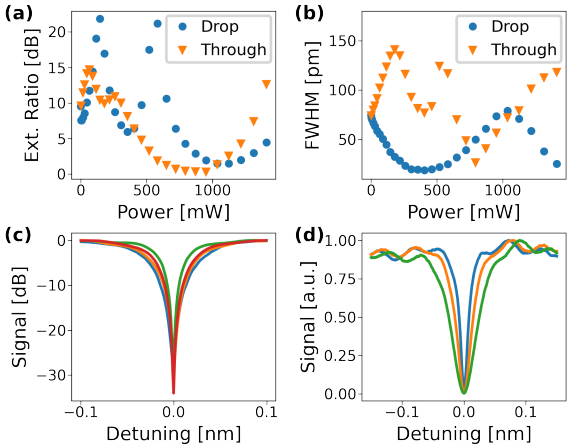

Fig. 5: (a) Extinction ratio and (b) FWHM at different TOPS powers at the through- (blue dots) and drop-side (orange triangles) couplers. (c) High ER resonances for different applied voltages V_D. The resonant wavelengths and applied voltages are: 1503.0 nm at $V_D = 13$ V (blue), 1545.8 nm at $V_D = 28$ V (orange), 1576.2 nm at $V_D = 6$ V (green) and 1588.0 nm at 6 V (red). (d) Resonance at λ_0 = 1550.2 nm resonance at $V_T = 0$ V, $V_D = 14.7$ V (blue), $V_T = 5$ V, $V_D = 13.5$ V (orange) and $V_T = 6.7$ V, $V_D = 11.7$ V (green).

By simultaneously tuning both interferometric coupling segments with different voltages V_T and V_D we were able to independently tune the ER and FWHM. Figure 5(d) shows a resonance at λ_0 = 1550.2 nm for three different combinations of voltages. All three measurements show an extinction ratio above 15 dB at FWHMs of 15.0 pm (blue curve), 27.2 pm (orange curve) and 44.8 pm (green curve). Thus the FWHM is tuned without reducing the extinction ratio of the resonance.

Conclusion

We have demonstrated a reconfigurable integrated LNOI racetrack resonator and showed extinction ratios as high as 34 dB at different wavelengths throughout the S-, C- and L-band. Furthermore, simultaneous and independent tuning of the extinction ratio, FWHM and resonance position was achieved. In particular, the FWHM was tuned between 15 pm and 45 pm while keeping the extinction above 15 dB. These integrated devices are a promising tool for enhancing nonlinear optical effects as they relax fabrication tolerances on the coupling segments and allow to use the same resonator in different coupling regimes. Introducing air-trenches into the design would drastically reduce the power consumption of the TOPS[17],[21].

Acknowledgements

We acknowledge the support for nanofabrication from ScopeM, BRNC, and FIRST of ETH Zürich and funding from SNSF BRIDGE Discovery 194693.

References

[1] L. Zhang, L. Jie, M. Zhang, Y. Wang, Y. Xie, Y. Shi, and D. Dai, "Ultrahigh-Q silicon racetrack resonators", *Photonics Research*, vol. 8, no. 5, pp. 684–689, May 2020. DOI: 10.1364/PRJ.387816.

[2] X. Ji, S. Roberts, M. Corato-Zanarella, and M. Lipson, "Methods to achieve ultra-high quality factor silicon nitride resonators", *APL Photonics*, vol. 6, no. 7, p. 071 101, 2021. DOI: 10.1063/5.0057881.

[3] M. Zhang, C. Wang, R. Cheng, A. Shams-Ansari, and M. Lončar, "Monolithic ultra-high-Q lithium niobate microring resonator", *Optica*, vol. 4, no. 12, pp. 1536–1537, 2017. DOI: 10.1364/OPTICA.4.001536.

[4] D. Liang, X. Huang, G. Kurczveil, M. Fiorentino, and R. G. Beausoleil, "Integrated finely tunable microring laser on silicon", *Nature Photonics*, vol. 10, no. 11, pp. 719–722, 2016. DOI: 10.1038/nphoton.2016.163.

[5] Y. Liu, X. Yan, J. Wu, B. Zhu, Y. Chen, and X. Chen, "On-chip erbium-doped lithium niobate microcavity laser", *Science China Physics, Mechanics & Astronomy*, vol. 64, no. 3, Oct. 2020. DOI: 10.1007/s11433-020-1625-9.

[6] X. Xue, Y. Xuan, C. Wang, P.-H. Wang, Y. Liu, B. Niu, D. E. Leaird, M. Qi, and A. M. Weiner, "Thermal tuning of kerr frequency combs in silicon nitride microring resonators", *Optics express*, vol. 24, no. 1, pp. 687–698, 2016. DOI: 10.1364/OE.24.000687.

[7] H. Weng, J. Liu, A. A. Afridi, J. Li, J. Dai, X. Ma, Y. Zhang, Q. Lu, J. F. Donegan, and W. Guo, "Directly accessing octave-spanning dissipative kerr soliton frequency combs in an AlN microresonator", *Photonics Research*, vol. 9, no. 7, pp. 1351–1357, 2021. DOI: 10.1364/PRJ.427567.

[8] X. Zheng, E. Chang, P. Amberg, I. Shubin, J. Lexau, F. Liu, H. Thacker, S. S. Djordjevic, S. Lin, Y. Luo, *et al.*, "A high-speed, tunable silicon photonic ring modulator integrated with ultra-efficient active wavelength control", *Optics express*, vol. 22, no. 10, pp. 12 628–12 633, 2014. DOI: 10.1364/OE.22.012628.

[9] H. Li, G. Balamurugan, M. Sakib, J. Sun, J. Driscoll, R. Kumar, H. Jayatilleka, H. Rong, J. Jaussi, and B. Casper, "A 112 Gb/s PAM4 silicon photonics transmitter with microring modulator and CMOS driver", *Journal of Lightwave Technology*, vol. 38, no. 1, pp. 131–138, 2020. DOI: 10.1364/JLT.38.000131.

[10] Z. Yang, P. Chak, A. D. Bristow, H. M. van Driel, R. Iyer, J. S. Aitchison, A. L. Smirl, and J. Sipe, "Enhanced second-harmonic generation in AlGaAs microring resonators", *Optics letters*, vol. 32, no. 7, pp. 826–828, 2007. DOI: 10.1364/OL.32.000826.

[11] J. Lu, J. B. Surya, X. Liu, A. W. Bruch, Z. Gong, Y. Xu, and H. X. Tang, "Periodically poled thin-film lithium niobate microring resonators with a second-harmonic generation efficiency of 250,000%/W", *Optica*, vol. 6, no. 12, pp. 1455–1460, 2019. DOI: 10.1364/OPTICA.6.001455.

[12] J. Lu, A. Al Sayem, Z. Gong, J. B. Surya, C.-L. Zou, and H. X. Tang, "Ultralow-threshold thin-film lithium niobate optical parametric oscillator", *Optica*, vol. 8, no. 4, pp. 539–544, 2021. DOI: 10.1364/OPTICA.418984.

[13] J. E. Castro, T. J. Steiner, L. Chang, Q. Dang, W. Xie, C. Li, J. Norman, J. E. Bowers, and G. Moody, "Time-energy entangled photon pairs generated via SFWM in an AlGaAsOI ring resonator", in *Optical Fiber Communication Conference (OFC) 2021*, Optica Publishing Group, 2021, M3B.1. DOI: 10.1364/OFC.2021.M3B.1.

[14] Di Zhu, L. Shao, M. Yu, R. Cheng, B. Desiatov, C. Xin, Y. Hu, J. Holzgrafe, S. Ghosh, A. Shams-Ansari, *et al.*, "Integrated photonics on thin-film lithium niobate", *Advances in Optics and Photonics*, vol. 13, no. 2, pp. 242–352, 2021. DOI: 10.1364/AOP.411024.

[15] Y. Zhao, J. K. Jang, Y. Okawachi, and A. L. Gaeta, "Theory of $\chi(2)$-microresonator-based frequency conversion", *Optics Letters*, vol. 46, no. 21, pp. 5393–5396, 2021. DOI: 10.1364/OL.427684.

[16] A. Yariv, "Critical coupling and its control in optical waveguide-ring resonator systems", *IEEE Photonics Technology Letters*, vol. 14, no. 4, pp. 483–485, 2002. DOI: 10.1109/68.992585.

[17] X. Liu, P. Ying, X. Zhong, J. Xu, Y. Han, S. Yu, and X. Cai, "Highly efficient thermo-optic tunable micro-ring resonator based on an LNOI platform", *Optics letters*, vol. 45, no. 22, pp. 6318–6321, 2020. DOI: 10.1364/OL.410192.

[18] M. Mahmoud, L. Cai, C. Bottenfield, and G. Piazza, "Lithium niobate electro-optic racetrack modulator etched in Y-cut lnoi platform", *IEEE Photonics Journal*, vol. 10, no. 1, pp. 1–10, 2018. DOI: 10.1109/JPHOT.2018.2797244.

[19] I. Krasnokutska, J.-L. J. Tambasco, and A. Peruzzo, "Tunable large free spectral range microring resonators in lithium niobate on insulator", *Scientific reports*, vol. 9, no. 1, pp. 1–7, 2019. DOI: 10.1038/s41598-019-47231-3.

[20] L. Chen, N. Sherwood-Droz, and M. Lipson, "Compact bandwidth-tunable microring resonators", *Optics letters*, vol. 32, no. 22, pp. 3361–3363, 2007. DOI: 10.1364/OL.32.003361.

[21] G. Chen, H.-L. Lin, J. D. Ng, and A. J. Danner, "Integrated thermally tuned mach-zehnder interferometer in Z-cut lithium niobate thin film", *IEEE Photonics Technology Letters*, vol. 33, no. 13, pp. 664–667, Jul. 2021. DOI: 10.1109/lpt.2021.3086850.